AD-A089 843 MARYLAND UNIV COLLEGE PARK COMPUTER SCIENCE CENTER F/G 9/2
STOCHASTIC MODELS FOR CLOSED BOUNDARY ANALYSIS: PART I. REPRESE--ETC(U)
JUL 80 R L KASHYAP, R CHELLAPPA AFOSR-77-3271
UNCLASSIFIED TR-909 AFOSR-TR-80-0946 NL

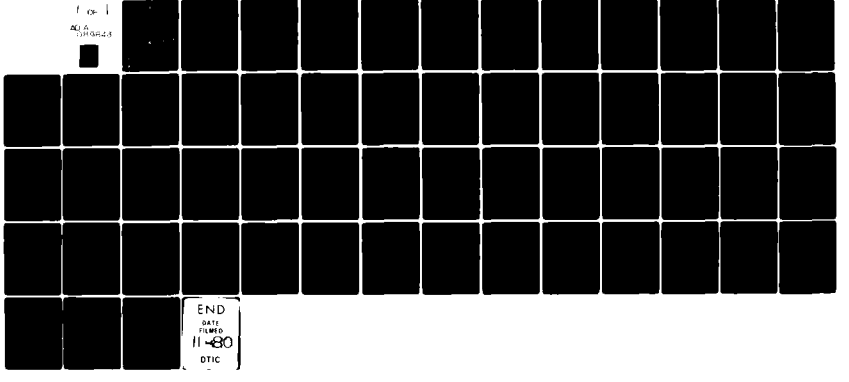

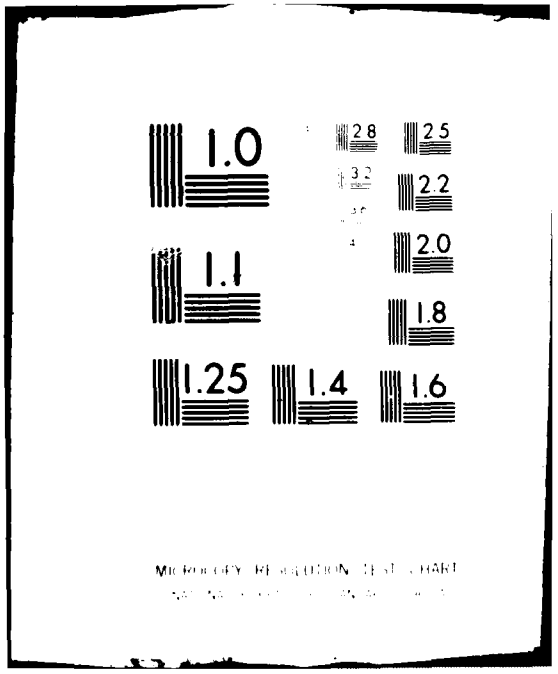
1.0
2.8
2.5
3.2
2.2
1.1
2.0
1.8
1.25
1.4
1.6

LEVEL II

12 P.S.

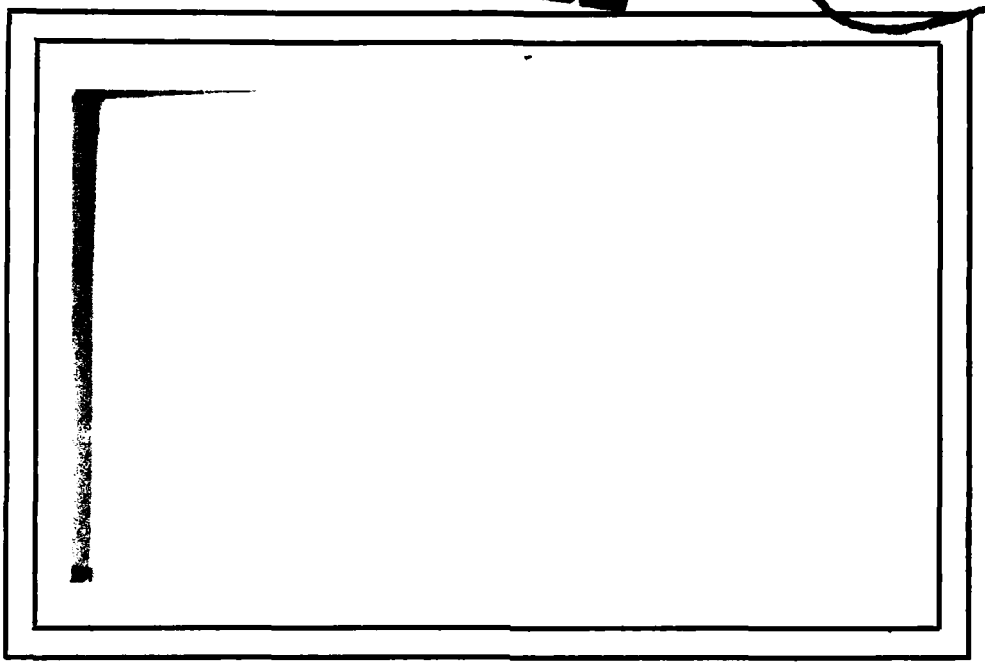

UNIVERSITY OF MARYLAND
COMPUTER SCIENCE CENTER

COLLEGE PARK, MARYLAND
20742

AIR FORCE OFFICE OF SCIENTIFIC RESEARCH (AFSC)
NOTICE OF TRANSMITTAL TO DDC
This technical report has been reviewed and is approved for public release IAW AFR 190-12 (7b).
Distribution is unlimited.
A. D. BLOSE
Technical Information Officer

TR-909
AFOSR-77-3271

July 1980

STOCHASTIC MODELS FOR CLOSED BOUNDARY ANALYSIS: PART I - REPRESENTATION AND RECONSTRUCTION

R. L. Kashyap*
R. Chellappa*,+

ABSTRACT

This paper deals with the analysis of closed boundaries of arbitrary shape in a plane. Specifically, it is concerned with the problems of representation and reconstruction. We first set up a one to one correspondence between the given closed boundary and a univariate or multivariate sequence of real numbers. Univariate or multivariate circular autoregressive models are suggested for the representation of the sequence of numbers derived from the closed boundary. The stochastic model representing the closed boundary is invariant to transformations of the boundary such as scaling, rotation and choice of the starting point. Methods for estimating the unknown parameters of the model are given and a decision rule for choosing the appropriate order of the model is included. Constraints on the estimates are derived so that the estimates are invariant to transformations of the boundaries. The specific stochastic model used enables us to reconstruct a closed boundary with less computational effort using FFT algorithms. Results of simulations are included and applications to contour coding are discussed. In a subsequent paper we will consider the classification problem.

*School of Electrical Engineering, Purdue University, West Lafayette, IN 47907. Supported in part by the National Science Foundation under Grant No. ENG-78-18271.

+Computer Science Center, University of Maryland, College Park, MD 20742. Supported in part by the Air Force Office of Scientific Research under Grant AFOSR-77-3271. The continued interest and encouragement of Prof. Azriel Rosenfeld is gratefully acknowledged.

1. Introduction

The problems of closed boundary analysis and discrimination are familiar in pattern recognition. They arise in a variety of situations such as contour coding [1,2], classification of chromosomes [3], interpretation of chest x-rays [4], scene analysis [5], and the detection of parts in a bin in robotics [6]. In this first part of our study of the applicability of stochastic models to such problems, we consider the analysis of boundaries. In a subsequent paper, classification of a closed boundary as one of several mutually exclusive boundaries will be considered. Specifically, in this paper we consider the problems associated with the representation and reconstruction of closed boundaries.

The statistical approach to shape analysis has so far been concerned with the Fourier analysis of some function derived from the boundary [7-10]. This is essentially a deterministic approach. Moreover, in practical applications, the Fourier series expansion is truncated to a certain number of terms, leading to an inexact representation of the data. Further, not all Fourier descriptions yield coefficients which are insensitive to rotation, scaling and variability in the starting point in the tracing of the boundary [7] and the coefficients do not always regenerate a closed boundary [8].

In this paper we suggest a stochastic model of a special type, the so-called Circular AutoRegressive (CAR) models, to

describe the data from the boundary. The given boundary is approximated by a series of straight line segments and the two-variable data formed by the (x,y) co-ordinates of the end points of the line segments denoted as $\{x_1(i),x_2(i)\}$, $i = 1,2,\ldots,N$, are used for the representation. One of the characteristics of the data is its circularity, i.e., $x_1(t+N) = x_1(t)$, $x_2(t+N) = x_2(t)$. For the class of objects in which each of N radii vectors from the centroid of the boundary intersect the boundary at only one point, a simple version of the two-dimensional representation is used, i.e., a one-dimensional series of real numbers is formed by measuring the lengths of successive radii vectors that are angularly equispaced. The observations $\{r(1),\ldots,r(N)\}$ again possess the circularity property.

The observation set, be it one-dimensional or two-dimensional, is represented by CAR models characterized by a set of unknown parameters. By making suitable assumptions about the noise driving the model, expressions are obtained for the maximum likelihood (m.l.) estimates of the parameters of the model. In actual applications, the so-called least square estimates are used which are an approximation to the m.l. estimates. The conditions for these estimates to be invariant to scaling, translation and starting point on the boundary are derived. It also turns out that these estimates are the sufficient statistics for the unknown parameters. We also consider the reconstruction problem and present algorithms for generating a closed contour. The CAR models yield the reconstruction of a closed curve in O(NlogN)

operations. The data compression aspects of the model are considered with specific applications such as the archival storage of weather maps [22] and contours.

The organization of the paper is as follows: Section 2 describes the different ways of obtaining suitable representations from a closed boundary. The general representation suggested is two-dimensional and is applicable to all closed boundaries in a plane. A one-dimensional representation is used for the class of objects in which each of the N radii vectors intersect the boundary at only one point. In later sections all the analytical results are obtained for the case of a one-dimensional model, which can be easily generalized to two-dimensional representations. The mathematical model is introduced in Section 3 and the properties possessed by the estimates of the parameters characterizing the model are described in Section 4. A decision rule to choose appropriate neighbors is also given. In Section 5 the coding of closed boundaries is considered. Results of the simulation are given in Section 6. Discussion is given in Section 7. Main results are stated as theorems, the proofs being given in the appendix.

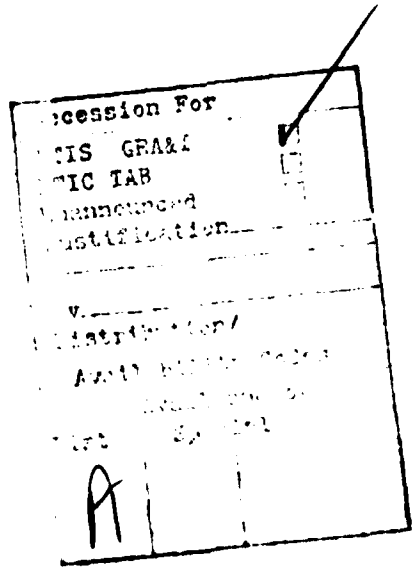

2. Representation of Closed Boundaries

We will represent the given closed boundary by a finite sequence of real numbers, the so-called time series. We assume that the boundary has no crossovers. We first approximate the boundary by a polygon of N sides. The time series exactly represents the polygon, i.e., given the time series, we can reconstruct the polygon, and vice versa. We can choose the integer N large enough to obtain the desired accuracy of approximation. We emphasize that the time series is constructed such that the corresponding shape analysis and classification rules are invariant to transformations of the boundary such as translation, scaling, rotation and the starting point in the tracing of the boundary. We now describe several methods of obtaining the time series from the boundary.

Method 1 (Two-Dimensional): Consider a Cartesian co-ordinate system such that the origin is at the centroid of the object. Let $\{x_1(i), x_2(i)\}$, $i = 1,2,\ldots,N$, represent the co-ordinates of a large number (say) N of points on the boundary as in Fig. 1. The required representation is $\{(x_1(i),x_2(i)), i = 1,2,\ldots,N\}$.

Method 2 (One-Dimensional): Let $\{(x_1(i),x_2(i)), i = 1,2,\ldots,N\}$ be the coordinates of a large number, say N, of points on the boundary. Let

$$x_1(0) = (1/N) \sum_{i=1}^{N} x_1(i), \quad x_2(0) = (1/N) \sum_{i=1}^{N} x_2(i)$$

and let $(x_1(0),x_2(0))$ be denoted as the origin 0. Let A_1 be any point on the boundary. Mark off (N - 1) points $A_2,A_3,\ldots,A_N$ such that the angles between $0A_i$ and $0A_{i+1}$ are all the same, viz., $(2\pi/N)$ radians. This is shown in Fig. 2. Let the distance $0A_i = r(i)$, $i = 1,2,\ldots,N$. The required polygon is $A_1,A_2,\ldots,A_N$, and the time series is $\{r(1),r(2),\ldots,r(N)\}$.

Method 3 (One-Dimensional): We can construct the points $A_1,\ldots,A_N$ as in Method 2. Let the distance between A_i and A_{i+1} be $b(i)$, $i = 1,2,\ldots,N-1$. $b(N)$ is the distance between A_N and A_1. The required time series is $\{b(1),b(2),\ldots,b(N)\}$.

Method 4 (One-Dimensional): We fit a polygon of N sides to the boundary such that all the sides have the same length. Call the polygon $A_1A_2\ldots A_NA_1$. Let ϕ_i be the angle between A_iA_{i+1} and a reference line. Then $\{\phi_i, i = 1,2,\ldots,N\}$ is the required time series.

Note that methods 2, 3 and 4 can be used to represent what we shall call Type 1 objects. The class of Type 1 objects include non-convex objects as in Figure 2.

Definition (Type 1):

In any type 1 object the N radii vectors from the centroid of the object intersect the boundary at only one point.

Another possible representation for closed boundaries is the tangent angle versus arc length [8]. One disadvantage of this representation is that the angle function is more sensitive to the noise inherent in a fuzzy boundary. The angle function is related to the derivative of the coordinate function, and hence small variations in the co-ordinate values of the boundary points can result in large variations in the direction of the tangent vector.

3. Mathematical Modeling of Boundaries

Henceforth, we consider the analysis with respect to the one-dimensional data $\{r(1),\ldots,r(N)\}$ derived by using Method 2. These results are generalizable to the two-dimensional representations of the non-Type 1 objects.

We are given a one-dimensional sequence $\{r(1),r(2),\ldots,r(N)\}$ such that

$$r(N+k) = r(k),\ k = 1,2,\ldots,N$$

$$r(-k) = r(N-k+1),\ k = 1,2,\ldots,N \qquad (3.1)$$

We will fit a particular type of stochastic process called a Circular AutoRegressive (CAR) Process as in (3.2):

$$r(t) = \alpha + \sum_{j=1}^{m} \theta_j r(t-t_j) = \sqrt{\beta}\omega(t),\ t = 1,\ldots,N \qquad (3.2)$$

where t_j, $j = 1,2,\ldots,m$ are positive integers,

$$\omega(N+t) = \omega(t),\ t = 1,2,\ldots,N,$$

$$E(\omega(i)) = 0,\ E(\omega(i)\omega(j)) = \beta\delta_{ij},\ 1 \le i,j \le N$$

$$\delta_{ij} \neq 0 \text{ if } i = j$$

$$= 0 \text{ otherwise,}$$

$\omega(\cdot)$ is independent and normal $(0,\beta)$ and $\{\alpha,\theta_1,\ldots,\theta_m,\beta\}$ are unknown.

A similar stochastic model is used for both co-ordinates of the two-dimensional representation, i.e.,

$$x_i(t) = \alpha_i + \sum_{j=1}^{m} \theta_{ij} x_i(t-t_{ij}) + \sqrt{\beta_i}\omega_i(t),\ i = 1,2$$

where $x_i(t+N) = x_i(t)$, $i = 1,2$ and $\{\omega_1(\cdot)\}$ and $\{\omega_2(\cdot)\}$ are two independent normal i.i.d. noise sequences. This simple extension of (3.2) will be used throughout for non-Type 1 objects. By introducing interdependence between $x_1(\cdot)$ and $x_2(\cdot)$ more general models can be considered.

Because of the circularity assumption, given $\omega(1),\ldots,\omega(N)$, we can obtain $r(1),\ldots,r(N)$ by solving the system of N equations in (m+1) variables given in (3.3):

$$\begin{bmatrix} 1 & -\theta_m & \cdots & -\theta_2 & -\theta_1 \\ -\theta_1 & 1 & -\theta_m & \cdots & -\theta_3 & -\theta_2 \\ -\theta_2 & -\theta_1 & 1 & \cdots & -\theta_4 & -\theta_3 \\ & & & & & \\ & & & & & \\ 0 & \cdots & -\theta_m & -\theta_{m-1} & -\theta_1 & 1 \end{bmatrix} \begin{bmatrix} r(1) \\ r(2) \\ \\ \\ r(N) \end{bmatrix} = \alpha \begin{bmatrix} 1 \\ 1 \\ \\ \\ 1 \end{bmatrix} + \sqrt{\beta} \begin{bmatrix} \omega(1) \\ \omega(2) \\ \\ \\ \omega(N) \end{bmatrix} \qquad (3.3)$$

or equivalently,

$$B(\theta)\underset{\sim}{R} = \underset{\sim}{A} + \sqrt{\beta}\underset{\sim}{W}$$

where $\underset{\sim}{R} = [r(1),\ldots,r(N)]^T$

$\underset{\sim}{A} = [\alpha,\ldots,\alpha]^T$, Nx1 vector

$\underset{\sim}{W} = [\omega(1),\ldots,\omega(N)]^T$

$B(\theta)$= circulant $[1,0,0,\ldots,-\theta_m, -\theta_{m-1},-\theta_1]$.

$B(\theta)$ is a circulant matrix and it can be generated from its first row given above. The probability density of the set of observations is given in (3.4):

$$p(r(1),\ldots,r(N)|\alpha,\underset{\sim}{\theta},\beta)$$
$$= \det|B(\underset{\sim}{\theta})|\ [1/2\pi\beta]^{N/2} \exp\{(-1/2\beta)\sum_{t=1}^{N}(r(t) - \alpha - \theta^T z^T(t-1))^2\} \quad (3.4)$$

where $\underset{\sim}{\theta} = (\theta_1,\ldots,\theta_m)^T$

$\underset{\sim}{z}(t-1) = (r(t-t_1),\ r(t-t_2),\ldots,r(t-t_m))^T$

and $|\det B(\underset{\sim}{\theta})|$ is the Jacobian of the transformation from $r(1),\ldots,r(N)$ to $\omega(1),\ldots,\omega(N)$ and has the following expression [11] in view of the circulant structure of $B(\underset{\sim}{\theta})$:

$$|\det B(\underset{\sim}{\theta})| \triangleq |B(\underset{\sim}{\theta})| = \prod_{k=0}^{N-1}(1 - \underset{\sim}{\theta}^T\underset{\sim}{\psi}_k) \quad (3.5)$$

where the m-vector $\underset{\sim}{\psi}_k$ is as follows:

$$\underset{\sim}{\psi}_k = \text{column}\ [\exp(-\sqrt{-1}2\pi k t_i/N),\ i = 1,2,\ldots,m]$$

In our formulation, the shape of the boundary is controlled by the coefficients $(\alpha,\underset{\sim}{\theta},\beta)$. The random sequence $\omega(1),\omega(2),\ldots,\omega(N)$ represents the effect of noise on the boundary. For instance, given N i.i.d. random variables $\omega(1),\ldots,\omega(N)$ from a Gaussian or Gamma distribution, we can account for a class of shapes which are minor variations of the basic shape, the so-called local variations of the shape. On the other hand, global transformations like scaling and rotation of the given shape are controlled by the parameters $(\alpha,\underset{\sim}{\theta},\beta)$. Note that these global variations preserve the shape and the parameter sets $(\alpha,\underset{\sim}{\theta},\beta)$ corresponding to various shapes which are related to each other by transformations like scaling, rotation, translation and the starting point

are simply related by Theorem 1. On the other hand, the parameter sets of quite different shapes cluster in $(\alpha,\underset{\sim}{\theta},\beta)$ far apart. Fig. 3 illustrates some possible transformations of shapes. The constraint on the parameter set $(\alpha,\underset{\sim}{\theta},\beta)$ representing the class of shapes that result due to these transformations is given in Theorem 1.

Theorem 1: Consider a closed boundary represented by $r(1)$, $r(2),\ldots,r(N)$, obeying the following equation involving the coefficients $(\alpha,\underset{\sim}{\theta},\beta)$:

$$r(t) = \alpha + \sum_{i=1}^{m} \theta_i r(t-t_i) = \sqrt{\beta}\omega(t),\ t = 1,2,\ldots,N \qquad (3.6)$$

All other boundaries which have the same shape as the boundary represented by $r(1), r(2),\ldots,r(N)$ can be generated by equation (3.6) with the same $\omega(\cdot)$ and indexed by the coefficients $(\alpha',\underset{\sim}{\theta}',\beta')$ related to $(\alpha,\underset{\sim}{\theta},\beta)$ by (3.7):

$$\underset{\sim}{\theta}' = \underset{\sim}{\theta},\ \alpha'/\sqrt{\beta'} = \alpha/\sqrt{\beta} \qquad (3.7)$$

The proof is given in the appendix.

The significance of Theorem 1 is as follows: Given a shape and its scaled or rotated version, the corresponding values of $\underset{\sim}{\theta}$ and $\alpha/\sqrt{\beta}$ are identical. Or equivalently, similar shapes cluster closely in the (m+1) parameter space $(\underset{\sim}{\theta},\alpha/\sqrt{\beta})$. Allowing variations within a class of shapes due to noise, etc., we see that the parameters of the class of shapes will form a close cluster. This suggests the use of $\underset{\sim}{\phi} = (\underset{\sim}{\theta}^T,\alpha/\sqrt{\beta})^T$ as the

feature vector for classification of shapes. This will be considered in detail in a subsequent paper.

4. Parameter Estimation and the Properties of the Estimates

The unknown parameters $(\alpha,\underset{\sim}{\theta},\beta)$ in the model in (3.2) are estimated from the observed time series taken from a given boundary. The popular method of estimation of parameters is the maximum likelihood estimate (m.l.e). The m.l.e. denoted by $(\alpha^*,\underset{\sim}{\theta}^*,\beta^*)$ is the value of $(\alpha,\underset{\sim}{\theta},\beta)$ which maximizes $p(r(1),\ldots, r(N)|\alpha,\underset{\sim}{\theta},\beta)$. The estimates are given in Theorem 2.

Theorem 2: Let $(\alpha^*,\underset{\sim}{\theta}^*,\beta^*)$ be the maximum likelihood estimates of the parameters $(\alpha,\underset{\sim}{\theta},\beta)$. Then

$$\underset{\sim}{\theta}^* = \text{Arg}\left[\min_{\underset{\sim}{\theta}\in R^m}\left\{-\sum_{k=0}^{N-1}\ell n(1-\underset{\sim}{\theta}^T\underset{\sim}{\psi}_k) + N/2\ \ell n\sum_{t=1}^{N}(r(t)-\underset{\sim}{\theta}^T\underset{\sim}{z}(t-1)-\alpha(\underset{\sim}{\theta}))^2\right\}\right] \tag{4.1}$$

where

$$\alpha(\underset{\sim}{\theta}) = 1/N\sum_{t=1}^{N}(r(t)-\underset{\sim}{\theta}^T\underset{\sim}{z}(t-1))$$

$$\alpha^* = \alpha(\underset{\sim}{\theta}^*) = 1/N\sum_{t=1}^{N}(r(t)-\underset{\sim}{\theta}^{*T}\underset{\sim}{z}(t-1)) \tag{4.2}$$

and

$$\beta^* = 1/N\sum_{t=1}^{N}(r(t)-\alpha^*-\underset{\sim}{\theta}^{*T}\underset{\sim}{z}(t-1))^2 \tag{4.3}$$

The proof is given in the appendix.

$\underset{\sim}{\theta}^*$ can be computed by a gradient algorithm. For reduced computations we suggest the use of the least square (l.s.) estimates given below:

$$(\bar{\underset{\sim}{\theta}}^T, \bar{\alpha})^T = \left[\sum_{t=1}^{N} \underset{\sim}{u}(t-1)\underset{\sim}{u}^T(t-1)\right]^{-1} \left[\sum_{t=1}^{N} \underset{\sim}{u}(t-1)r(t)\right] \quad (4.4)$$

and

$$\bar{\beta} = (1/N) \sum_{t=1}^{N} (r(t) - (\bar{\underset{\sim}{\theta}}^T, \bar{\alpha})\underset{\sim}{u}(t-1))^2 \quad (4.5)$$

Also, $\bar{\alpha}$ can be written as

$$\bar{\alpha} = 1/N \sum_{t=1}^{N} (r(t) - \bar{\underset{\sim}{\theta}}^T \underset{\sim}{z}(t-1)) \quad (4.6)$$

where

$$\underset{\sim}{z}(t-1) = (r(t-t_1),\ldots,r(t-t_m))^T$$

The l.s. estimates can be interpreted as obtained by maximizing $p(r(1),\ldots,r(N)|\alpha,\underset{\sim}{\theta},\beta)$, with the determinant term $|B(\underset{\sim}{\theta})|$ in (3.4) suppressed. Since the relevant matrix $B(\underset{\sim}{\theta})$ is nearly lower triangular for large N, the l.s. estimates tend to m.l. estimates asymptotically. However, the easily computable l.s. estimates also possess invariance properties w.r.t. transformations like rotation, scaling and starting point. Numerical

simulations indicate that the error in the estimates due to the suppression of the determinant term is negligible. The details of the simulations are given in Section 6.

We make a brief note regarding the estimation of parameters when the two-dimensional representation is used for objects. By making the simplifying assumption of independence of the set of observations $\{x_1(\cdot)\}$ and $\{x_2(\cdot)\}$, the above mentioned methods of estimation are directly applicable. More details on the estimation of parameters for vector processes can be found in [12].

In Theorem 1 we considered the constraints imposed on the parameter sets representing the class of shapes that result due to the transformations of shape. But in practice we work with only the estimates of the parameters. It is then necessary to consider the constraints imposed on the estimates of the parameter sets from the shapes that result due to transformations like scaling, rotation, etc. The properties possessed by the estimates can be broadly classified as those related to the shape and those related to the statistics of the data derived from the shape. For instance, the invariance of $(\bar{\theta}, \bar{\alpha}/\sqrt{\beta})$ under transformations like scaling and rotation are shape related properties, and the sufficiency property of the estimates comes under the other category. The estimate $(\bar{\theta}, \bar{\alpha}/\sqrt{\beta})$ possesses the following properties:

P1) Invariance to scaling of the boundary.

P2) Invariance to variation in the starting point used in tracing the boundary.

P3) Invariance to rotation of the boundary.

P4) Invariance to translation of the boundary.

P5) The l.s. estimates are a sufficient statistic for the unknown parameters.

The method of tracing the boundary in the one-dimensional representation is such that an effective normalization is done w.r.t. the center of gravity of the shape. Thus the one-dimensional representation is invariant to translation. Since the origin of the two-dimensional co-ordinate system is fixed at the centroid of the object in Method 1, this representation is also independent of translation.

Also, since we go around the boundary once completely, and use the entire observation set in estimating the parameters, the effect of rotation of the axes and the effect due to the variation in the starting point are the same.

Theorem 3: Let $(\bar{\alpha},\bar{\underset{\sim}{\theta}},\bar{\beta})$ denote the estimates of the parameters of the model representing a Type 1 object and let $(\bar{\alpha}_1,\bar{\underset{\sim}{\theta}}_1,\bar{\beta}_1)$ and $(\bar{\alpha}_2,\bar{\underset{\sim}{\theta}}_2,\bar{\beta}_2)$ represent the corresponding estimates of the model representing a non-Type 1 object. Then the estimates $(\bar{\theta},\bar{\alpha}/\sqrt{\bar{\beta}})$ and $\{(\theta_1,\alpha_1/\sqrt{\bar{\beta}_1}),\ (\theta_2,\alpha_2/\sqrt{\bar{\beta}_2})\}$ satisfy the properties P1-P4. The proof of Theorem 3 is given in the appendix.

We state a theorem below regarding P5. A proof similar to the one found in [13] can be given for this theorem.

Theorem 4: The l.s. estimates $(\bar{\alpha},\underset{\sim}{\bar{\theta}},\bar{\beta})$ are sufficient statistics for the unknown parameters $(\alpha,\underset{\sim}{\theta},\beta)$.

There are two consequences resulting from the existence of sufficient statistics for the parameters $(\alpha,\underset{\sim}{\theta},\beta)$. The first consequence is that all the information contained in the unknown parameters $(\alpha,\underset{\sim}{\theta},\beta)$ is also contained in the estimates $(\bar{\alpha},\underset{\sim}{\bar{\theta}},\bar{\beta})$.

The second consequence is that $(\bar{\alpha},\underset{\sim}{\bar{\theta}},\bar{\beta})$ is the optimal feature set for classification purposes [13]. Hence, we can restrict our attention to a class of decision rules that are functions of sufficient statistics. This will be further considered in a subsequent paper.

Choice of the number of lag terms: We have so far done the analysis as though the number of lag terms in eq. (3.2) is known. As mentioned in Section 3, we need not have all the lag terms up to the highest lag term, the lag terms present being indicated by the set $\{t_i\}$. The problem of determining the number of lag terms comes under a general class of problems known as "system identification" and has been considered elsewhere [14]. Without going into the details we simply formulate the problem and give a decision rule to choose the best m for the given boundary.

Suppose that we consider three possible values of m, m_1, m_2, and m_3. Corresponding to each m_i, i = 1, 2, 3, we will write the corresponding circular autoregressive equation E_i, i = 1, 2, 3:

$$E_i: r(t) = \alpha_i + \sum_{j=1}^{m_i} \theta_{ij} r(t - t_{ij}) + \sqrt{\beta_i}\,\omega(t),$$

$$t = 1,2,\ldots,N,\ i = 1,2,3 \qquad (4.7)$$

$$\underset{\sim}{\theta}_i = (\theta_{i1},\ldots,\theta_{im_i})^T,\ \theta_{ij} \neq 0,\ \forall_j = 1,2,\ldots,m_i$$

$\beta_i > 0,\ i = 1, 2, 3$

The lag terms $\{t_{ij}\}$ differ from model to model.

We only know that $r(\cdot)$ obeys one of the given equations E_i. Note that the equations are mutually exclusive. We can use the standard Bayesian methods [13] to obtain a decision rule. The simplified decision rule is given below. Compute the statistics C_k, $k = 1, 2, 3$:

$$C_k = N\ell n\beta_k + \sum_{i=0}^{N-1} \ell n(1 - \overline{\underset{\sim}{\theta}}^T \underset{\sim}{\psi}_i) + m_k f_i(N) \qquad (4.8)$$

where $\overline{\beta}, \overline{\underset{\sim}{\theta}}$ are defined in (3.10) and (3.12) and $f_i(N)$ is some suitable function of N. Typically, $f_i(N)$ could be ℓnN [14], or 0.01. The decision rule to choose the appropriate m_i is as follows: Choose the model k* if

$$k^* = \arg\min_k \{C_k\} \qquad (4.9)$$

The choice of $f_i(N)$ in (4.8) is a tradeoff between the two types of errors that arise in a hypothesis testing problem. Consider the case of choosing between a m^{th} and an $(m+1)^{st}$ order model. Then it can be shown that the probability of choosing the lower order model when indeed the higher order model is true

(the so-called Type II error) is proportional to $\sqrt{f_i(N)}$. When the primary interest is to reconstruct the shape, a higher order model is preferred and it is important to keep the Type II error under control. For this reason, $f_i(N)$ should be 0.01 or smaller.

5. Coding and Reconstruction Schemes

In this section we discuss the coding and reconstruction schemes possible with the circular model developed in this paper. We consider the applicability of such schemes to a class of two tone images [2] like weather maps and geographical contours, typical illustrations of which are shown in Fig. 4.

The given closed contour is represented by a model similar to (3.2). The estimates of the parameters characterizing the model and the residuals defined as

$$\bar{\omega}(t) = (1/\sqrt{\bar{\beta}})[r(t) - \bar{\alpha} - \sum_{j=1}^{m} \bar{\theta}_j r(t - t_j)] \qquad (5.1)$$

are computed. The CAR model considered in this paper splits the information contained in the original correlated observations into two sets: the statistical information contained in the set $(\alpha, \underset{\sim}{\theta}, \beta)$ and the information contained in the uncorrelated residuals. The former set characterizes a class of shapes with different noise sequences while the combined set $(\bar{\alpha}, \underset{\sim}{\bar{\theta}}, \bar{\beta}, \bar{\omega}(1), \ldots, \bar{\omega}(N))$ represents a particular realization of the shape. In actual implementation the exact residuals are never stored. Either they are truncated or truncated and skipped, i.e., some of the truncated residuals are replaced by those from a (0,1) Gaussian random generator. If the skipped and truncated residuals are denoted by $\{\hat{\omega}(\cdot)\}$ and $\{\omega'(\cdot)\}$ respectively and $\{v(\cdot)\}$ denote the (0,1) Gaussian random numbers then one method of generating $\{\hat{\omega}(\cdot)\}$ would be as in (5.2):

$$\hat{\omega}(2t) = \omega'(2t), \qquad t = 1,2,\ldots,N/2$$
$$\hat{\omega}(2t-1) = v(2t-1), \qquad t = 1,3,\ldots,N/2-1 \tag{5.2}$$
$$\hat{\omega}(2t+1) = \omega'(2t+1), \qquad t = 0,2,\ldots,N/2-2$$

In (5.2), every 1/4th of truncated residual is replaced by a (0,1) Gaussian random number. It is also possible to generate $\{\hat{\omega}(\cdot)\}$ where every other $\{\omega'(\cdot)\}$is replaced by $\{v(\cdot)\}$. The particular scheme is generally decided by the degree of approximation desired. Such trimmed residuals are quantized and stored. From this stored information a closed contour that is a good approximation to the original contour can be generated by the simultaneous scheme described below:

Simultaneous Scheme: Given N trimmed residuals $\{\hat{\omega}(\cdot)\}$, truncated or truncated and skipped, and the estimates $(\bar{\alpha},\underset{\sim}{\bar{\theta}},\bar{\beta})$, find $\hat{r}(i)$, $i = 1,2,\ldots,N$ such that the norm

$$||B(\underset{\sim}{\bar{\theta}})\underset{\sim}{R} - \underset{\sim}{\bar{A}} - \underset{\sim}{\hat{W}}||^2 \tag{5.3}$$

is minimized, where $\underset{\sim}{R}^T = (r(1),\ldots,r(N))$, $\underset{\sim}{\bar{A}}^T = [\bar{\alpha},\bar{\alpha},\ldots,\bar{\alpha}]$, Nx1 vector, and $\underset{\sim}{\hat{W}} = [\hat{\omega}(1),\ldots,\hat{\omega}(N)]^T$. An optimal solution that minimizes the expression in (5.3) is given in Theorem 5:

Theorem 5: Let $\hat{\omega}(1),\ldots,\hat{\omega}(N)$ be the trimmed residuals and $(\bar{\alpha},\underset{\sim}{\bar{\theta}},\bar{\beta})$ be the estimates of the parameters of the model. Let $\underset{\sim}{\hat{R}} = \text{Arg}\ \{\min_{\underset{\sim}{R}}\{||B(\underset{\sim}{\bar{\theta}})\underset{\sim}{R} - \underset{\sim}{A} - \sqrt{\bar{\beta}}\underset{\sim}{\hat{W}}||^2\}\}$. Then $\underset{\sim}{\hat{R}}$ can be computed as shown below:

$$\hat{r}(k) = \sum_{i=1}^{N} e^{j(2\pi/N)(i-1)(k-1)} u'(i),\ k=1,2,\ldots,N,\ j = \sqrt{-1} \quad (5.4)$$

where

$$u'(i) = u(i)/\lambda(i) \quad (5.5)$$

$$u(i) = 1/N \sum_{n=1}^{N} e^{-j(2\pi/N)(i-1)(n-1)} (\bar{\alpha} + \sqrt{\bar{\beta}}\hat{\omega}(n)),\ i=1,2,\ldots,N \quad (5.6)$$

$$\lambda(i) = (1 - \underset{\sim}{\theta}^T \underset{\sim}{\psi}_i),\ i = 1,2,\ldots,N \quad (5.7)$$

and

$$\underset{\sim}{\psi}_i^T = (e^{-j(2\pi/N)(i-1)t_1}, e^{-j(2\pi/N)(i-1)t_2}, \ldots, e^{-j(2\pi/N)(i-1)t_m})$$

The proof of Theorem 5 is given in the appendix.

Comments:

1) Reduction in the computations using FFT algorithms is possible due to the following:

   a) the eigenvalues of the circulant matrices can be written down by inspection from the first row of the matrix, and

   b) The eigenvectors of the circulant matrix are universal, i.e., all possible circulant matrices of a specified order have an identical set of Fourier eigenvectors.

2) Eq. (5.7) is of computational complexity O(N log N) and so is Eq. (5.9). Since other computations like Eq. (5.8) are of complexity O(N), the overall computational complexity is O(N log N).

Recursive Scheme: A recursive scheme similar to the DPCM scheme can be suggested for the reconstruction of contours. The estimates $(\bar{\alpha},\underset{\sim}{\bar{\theta}},\bar{\beta})$ and the truncated and quantized residuals are used in (3.2) along with m initial conditions to generate the synthetic observation set. Owing to the uncorrelated nature of the residuals considerable saving in bits can be achieved. If exact residuals are used the original closed contour can be generated but in practice the exact residuals are never stored. Only truncated and quantized residuals are stored. Depending on the particular truncation and quantization schemes, contours that are close enough to the original contours can be generated.

6. Results of Simulation

In this section we summarize the results of simulations done with three closed boundaries shown in Fig. 5, denoted as shapes A, B, and C. Shapes A and C are typical Type 1 objects and shape B is a typical non-Type 1 object.

6.1 Model Order Selection: The decision rule in (4.9) was used to choose an appropriate model for different values of $f_i(N)$. The model orders chosen for different values of $f_i(N)$ for shapes A and C are given in Table 1.

Table 1. Model orders for different $f_i(N)$ in (4.8).

$f_i(N)$	MODEL ORDER CHOSEN	
	SHAPE A	SHAPE C
0.01	13	15
0.1	13	15
1.0	12	6
1.2	6	6
1.5	2	2
2.0	2	2

As discussed before by decreasing $f_i(N)$ we reduce the probability of choosing a lower order model when the higher order

model is true. It is this error that is crucial for applications like reconstruction. The value of $f_i(N)$ is chosen depending on the quality of reconstruction desired.

6.2 Accuracy of the least square estimates: To check the accuracy of the l.s. estimates as compared to m.l. estimates, the relative contributions of the first term and the quadratic term in (4.1) to the log likelihood function $\ell np(r(1),\ldots,r(N)|\alpha,\underset{\sim}{\theta},\beta)$ were computed for shapes A and C, for a twelfth order model, and are given in Table 1. It is seen that the contribution of log $|\det B(\underset{\sim}{\theta})|$ is negligible compared to the other term.

Table 2. Relative contributions of the log linear term and the quadratic term in (4.1).

SHAPE	CONTRIBUTION DUE TO LOG LINEAR TERM IN (4.1)	CONTRIBUTION DUE TO QUADRATIC TERM IN (4.1)
A	.1590	24.96
C	-.2326	48.90

6.3 Reconstruction of boundaries: We give examples of the reconstruction of boundaries. Fig. 6 gives the results of simulation experiments with shape A. Since shape A is a Type 1 object the one-dimensional representation was used. Least square

estimates $(\bar{\alpha},\underset{\sim}{\bar{\theta}},\bar{\beta})$ were computed. In Fig. 6 all the closed contours have been reconstructed using the simultaneous scheme in Theorem 5. Fig. 6a is the shape reconstructed using a second order model and the exact residuals. Fig. 6b is the shape using the residuals truncated to the first decimal place. The quality of reconstruction is close to Fig. 6a. Figs. 6c and 6d are similar to Figs. 6a and 6b except that a twelfth order model has been used. All the shapes in Fig. 6 look very similar to the original shape A. Then the natural question is the relevance of the decision rule used in fitting an appropriate model. This is explained as follows: the residuals of an inappropriate model will not be as uncorrelated as those of an appropriate model and hence the efficiency of coding is higher when a model of the correct order is used. Since the data generated by the simultaneous model is circular we <u>always</u> reconstruct closed contours. Fig. 7 gives the same results as in Fig. 6 for shape B.

Fig. 8 gives the reconstructed shape A using the recursive scheme mentioned earlier. Fig. 8a and 8b are the results of this scheme with m = 2 and using the exact and the truncated residuals respectively. Though this scheme does not truly generate a closed contour (because of its recursive nature) still the quality of reconstruction is good. Figs. 8c and 8d are similar to 8a and 8b, with a twelfth order model. Fig. 9 gives the results for shape B. Fig. 9a and 9c are reconstructed using the exact residuals and m = 2 and 12. Fig. 9b is the

result of the recursive scheme with truncated residuals and m = 2. Note the presence of a spike, due to the noncircularity of the data. Similarly, Fig. 9d is the reconstruction with m = 12 and the resulting contour is not closed.

As mentioned before, the circular model splits the information in two parts, the estimates of parameters and the residuals. The information contained in the estimates represents a class of shapes corresponding to different i.i.d noise sequences. To see how much information is contained in the estimates, synthetic generation of shapes is attempted. The results are given in Fig. 10 for shape A. The residuals used were drawn from a (0,1) Gaussian random number generator. Fig. 10a and 10b are reconstructed with m = 2 and the recursive and simultaneous schemes respectively. Note that the recursive scheme does not generate closed contours. Figs. 10c and 10d are for m = 12. As expected, the quality of reconstruction with pseudo-random numbers is not as good as with exact residuals but the general shape is still recovered. Also note that models of order 12 generate contours that are much closer to the original than the contours generated by a model of order m = 2.

The coding schemes mentioned above can be used for the storage of contours as in Fig. 4. We fit a stochastic model to every closed contour, and store the estimates of the coefficients and the quantized residuals. For contours in the map

that are not closed, we can fit ordinary autoregressive models. The map can be reconstructed by reconstructing each contour separately.

7. Discussion

In this section we compare the theory developed here with other well-known methods like Fourier analysis [7-10,15]. The main emphasis of the theory developed here is to demonstrate that statistical methods can be developed to handle a wide class of closed boundaries.

In the familiar Fourier analysis method a continuous function is extracted from the boundary and represented as a Fourier series. These methods are basically deterministic compared to the stochastic models considered here. Generally stochastic models are found to be more useful in noisy situations and tend to describe the data by fewer parameters than the deterministic models [16]. In fact by using the theory of comparison of dynamic models [14], an exact comparison of the Fourier series representation and the stochastic model considered here can be made.

In any practical situation, the Fourier series expansion has to be truncated. Because of the truncation in the Fourier series representation, the data reduction from the observations to the Fourier coefficients is not exact. We have given a decision rule to choose the appropriate lag terms for the boundary analysis.

One of the criticisms of current boundary coding schemes [17, p. 161] is that the points (A,B) and (C,D) in Fig. 11 which are geometrically close together can be encoded quite far apart in the resulting string. Such boundaries can be adequately

represented by models which have non-contiguous lag terms [12]. Typically, such a model would include lag terms like $\{x_1(t-1),\ldots, x_1(t-N_1)\}$, where N_1 is the number of spaces between A and B.

The specific CAR model considered here, because of its circular nature, is intuitively pleasing for representing a closed boundary. The two-dimensional representation considered here is used to represent any closed curve on a plane, and the one-dimensional representation is used for the Type 1 objects. The time series is constructed such that the corresponding shape description is invariant to the transformations of the boundary. The vector $(\underset{\sim}{\bar{\theta}}, \bar{\alpha}/\sqrt{\bar{\beta}})$ is insensitive to these transformations of the shape and so is a natural choice for shape classification problems. We have suggested coding and reconstruction algorithms. The specific simultaneous reconstruction algorithm always results in a closed contour in O(NlogN) operations. We have also considered the problem of boundary coding for archival storage of weather maps and geographical maps. It is possible to extend these methods to two-dimensional images [18] where the edges are coded as contours.

Shape descriptors like ratio of square of perimeter to area [19] are not useful for synthesis of complicated shapes. Also they are not robust since they often yield similar numerical values for contours that are significantly different from one another [20], as shown in Fig. 9.

The theory developed here is based on a global description of shapes. In a subsequent paper (Part II), we will consider the problems of shape discrimination. In particular, we will be interested in obtaining decision rules that are invariant to transformations of shapes.

Appendix

We give the proofs of the various theorems given in the body of the paper.

Theorem 1: Given a closed boundary represented by {r(1), r(2),..., r(N)}, obeying the following equation involving the coefficients $(\alpha,\underset{\sim}{\theta},\beta)$,

$$r(t) = \alpha + \sum_{i=1}^{m} \theta_i r(t - t_i) + \sqrt{\beta}\omega(t), \quad t = 1,2,\ldots,N \qquad (1)$$

all other boundaries which have the same shape as the boundary represented by {r(1),...,r(N)}, can be generated by equation (1) with the same $\omega(1),\ldots,\omega(N)$ and the coefficients $(\alpha',\underset{\sim}{\theta}',\beta')$ related to $(\alpha,\underset{\sim}{\theta},\beta)$ by (2):

$$\underset{\sim}{\theta}' = \underset{\sim}{\theta}, \quad \alpha'/\sqrt{\beta'} = \alpha/\sqrt{\beta} \qquad (2)$$

Proof: Shape is preserved by the operations of scaling and rotation. We first consider the constraints imposed on the parameters to represent a class of shapes that differ due to scaling.

a) Scaling:

Any boundary which has the same shape as {r(·)}, but is scaled, is generated by {kr(1), kr(2),...,kr(N)}, where k is the scale factor, and obeys

$$kr(t) = \alpha' + \sum_{i=1}^{m} \theta_i' kr(t - t_i) + \sqrt{\beta'}\omega(t) \qquad (3)$$

or

$$r(t) = \alpha'/k + \sum_{i=1}^{m} \theta_i' r(t - t_i) + (\sqrt{\beta'}/k)\omega(t) \qquad (4)$$

Since r(t) obeys both (1) and (4), by the uniqueness of the solution of the difference equation, (2) follows.

b) Rotation: Consider the rotated boundary r'(1),...,r'(N), such that

$$r'(i) = r(i+S) \qquad (5)$$

and

$$\omega'(i) = \omega(i+S)$$

where S is a positive integer. Now

$$r'(t) = \alpha' + \sum_{i=1}^{m} \theta_i' r'(t - t_i) + \sqrt{\beta'}\omega'(t),\ t = 1,2,\ldots,N \qquad (6)$$

or

$$r(t + S) = \alpha' + \sum_{i=1}^{m} \theta_i' r(t - t_i + S) + \sqrt{\beta'}\omega(t + S),\ t = 1,2,\ldots,N$$

Equivalently,

$$r(k) = \alpha' + \sum_{i=1}^{m} \theta_i' r(k - t_i) + \sqrt{\beta'}\omega(k),\ k = 1+S,\ldots,S+N \quad (7)$$

(1) and (7) are identical and hence (2) follows.

Q.E.D.

Proof of Theorem 2: From (3.4), taking logarithms and using (3.5),

$$\ell np(r(1),\ldots,r(N)|\alpha,\underset{\sim}{\theta},\beta) = -N/2|n2\beta$$

$$- 1/2\beta \sum_{t=1}^{N} (r(t) - \underset{\sim}{z}^T(t-1)\underset{\sim}{\theta} - \alpha)^2 + \sum_{k=0}^{N-1} \ell n(1 - \underset{\sim}{\psi}_k^T\underset{\sim}{\theta}) \quad (8)$$

Differentiating w.r.t. α,β and equating to zero,

$$\alpha(\underset{\sim}{\theta}) = 1/N \sum_{t=1}^{N} (r(t) - \underset{\sim}{z}^T(t-1)\underset{\sim}{\theta})$$

$$\beta(\underset{\sim}{\theta}) = (1/N) \sum_{t=1}^{N} (r(t) - \underset{\sim}{z}^T(t-1)\underset{\sim}{\theta} - \alpha(\underset{\sim}{\theta}))^2 \quad (10)$$

Substituting (9) and (10) in (8) we have

$$\ell np(r(1),\ldots,r(N)|\alpha,\underset{\sim}{\theta},\beta) = -(N/2)|n(2\pi/N)$$

$$(-N/2)\ell n \sum_{t=1}^{N} [r(t) - \underset{\sim}{z}^T(t-1)\underset{\sim}{\theta} - \alpha(\underset{\sim}{\theta})]^2$$

$$+ \sum_{k=0}^{N-1} \ell n(1 - \underset{\sim}{\psi}_k^T\underset{\sim}{\theta}) - N/2$$

Maximizing $\ell n\ p(r(1),\ldots,r(N)|\alpha,\underset{\sim}{\theta},\beta)$ given above w.r.t. $\underset{\sim}{\theta}$ is equivalent to minimizing (4.1) w.r.t. $\underset{\sim}{\theta}$. Substituting the resulting $\underset{\sim}{\theta}^*$ in (9) and (10) we obtain Theorem 2.

Theorem 3: Let $(\bar{\alpha},\bar{\underset{\sim}{\theta}},\bar{\beta})$ denote the estimates of the parameters of the model representing a Type 1 object and let $(\bar{\alpha}_1,\bar{\underset{\sim}{\theta}}_1,\bar{\beta}_1)$ and $(\bar{\alpha}_2,\bar{\underset{\sim}{\theta}}_2,\bar{\beta}_2)$ represent the corresponding estimates of the model representing a non Type 1 object. Then the parameter sets $(\underset{\sim}{\theta}, \alpha/\sqrt{\beta})$ and $\{(\underset{\sim}{\theta}_1,\alpha_1/\sqrt{\beta}_1),\ (\underset{\sim}{\theta}_2,\alpha_2/\sqrt{\beta}_2)\}$ satisfy the properties P1-P4.

Proof: (a) Invariance to P1:

Let

$$r'(t) = kr(t),\ t = 1, 2,\ldots,N \tag{11}$$

be the scaled boundary.

Let the l.s. estimates of the parameters associates with $\{r'(\cdot)\}$, be $(\alpha',\underset{\sim}{\theta}',\beta')$.

From (4.4) and (11), it follows that $\underset{\sim}{\theta}' = \bar{\underset{\sim}{\theta}}$. Also from (4.5) and (4.6)

$$\alpha'/\sqrt{\beta'} = \frac{(1/N)\Sigma(r'(t) - \underset{\sim}{\theta}^T\underset{\sim}{z}'(t-1))}{\left[1/N \sum_{t=1}^{N} (r'(t) - \bar{\underset{\sim}{\theta}}^T\underset{\sim}{z}'(t-1) - \alpha(\bar{\underset{\sim}{\theta}}))^2\right]^{1/2}} = \bar{\alpha}/\sqrt{\bar{\beta}} \quad \text{using (11)}$$

(b) Invariance to P2: for this case $r'(t) = r(t+S)$ where S is the unit of rotation. By actually substituting in the expressions for $\underset{\sim}{\theta}'$ and $\alpha'/\sqrt{\beta'}$ and using

$$r(N+k) = r(k),$$

it is shown that $\underset{\sim}{\theta}' = \underset{\sim}{\bar{\theta}}$ and $\alpha'/\sqrt{\beta}' = \alpha/\sqrt{\beta}$.

Proof of Theorem 5:

From (5.3) we have

$$\underset{\sim}{\hat{R}} = B(\underset{\sim}{\bar{\theta}})^{-1}[\underset{\sim}{\bar{A}} + \sqrt{\beta}\ \underset{\sim}{\hat{W}}] \tag{12}$$

where $B(\underset{\sim}{\bar{\theta}})$ is a NxN circulant matrix. It is well known [11] that the eigenvectors of a NxN circulant matrix are the Fourier vectors $[\underset{\sim}{\phi}_1, \underset{\sim}{\phi}_2, \ldots, \underset{\sim}{\phi}_N]$, where ϕ_{ij}, the j^{th} component of the i^{th} eigenvector is given by

$$\phi_{ij} = e^{\sqrt{-1}(2\pi/N)(i-1)(j-1)} \tag{13}$$

and the distinct eigenvalues $\lambda(1), \ldots, \lambda(N)$ are given by

$$\lambda(k) = (1 - \underset{\sim}{\bar{\theta}}^T \underset{\sim}{\psi}_k) \tag{14}$$

$$\underset{\sim}{b} = [\underset{\sim}{\bar{A}} + \sqrt{\beta}\underset{\sim}{\hat{W}}] \tag{15}$$

Expanding $\underset{\sim}{b}$ in terms of the Fourier vectors $\{\underset{\sim}{\phi}_i\}$ we have

$$\underset{\sim}{b} = \sum_{i=1}^{N} \alpha_i \underset{\sim}{\phi}_i \tag{16}$$

where

$$\alpha_i = \underset{\sim}{\phi}_i^* \underset{\sim}{b}/N \tag{17}$$

and $\underset{\sim}{\phi}_i^*$ denotes the complex conjugate of $\underset{\sim}{\phi}_i^T$. Hence from (12), (15), (16), and (17)

$$\hat{\underset{\sim}{R}} = B(\bar{\underset{\sim}{\theta}})^{-1}\underset{\sim}{b} = B(\bar{\underset{\sim}{\theta}})^{-1}\sum_{i=1}^{N}\underset{\sim}{\phi}_i\underset{\sim}{\phi}_i^*\underset{\sim}{b}/N \tag{18}$$

Using

$$B(\underset{\sim}{\theta})^{-1}\underset{\sim}{\phi}_i = (1/\lambda(i))\underset{\sim}{\phi}(i)$$

the LHS of (18) is equal to

$$= \sum_{i=1}^{N}\underset{\sim}{\phi}_i\underset{\sim}{\phi}_i^*\underset{\sim}{b}/N\lambda(i) \tag{19}$$

Using (13), (14), and (19), the k^{th} component of $\hat{\underset{\sim}{R}}$ is

$$\hat{r}(k) = \sum_{i=1}^{N}\exp[\sqrt{-1}2\pi(i-1)(k-1)/N]/(1-\bar{\underset{\sim}{\theta}}^T\underset{\sim}{\psi}_i)$$

$$\left(\sum_{n=1}^{N}\exp[-\sqrt{-1}2\pi(i-1)(n-1)/N](\bar{\alpha}+\sqrt{\bar{\beta}}\hat{\omega}(n))\right) \tag{20}$$

Defining

$$u(i) = 1/N\sum_{n=1}^{N}\exp(-\sqrt{-1}2\pi(i-1)(n-1)/N)(\bar{\alpha}+\sqrt{\bar{\beta}}\hat{\omega}(n))$$

and

$$u'(i) = u(i)/(1-\underset{\sim}{0}^T\underset{\sim}{\psi}_i)$$

we have

$$\hat{r}(k) = \sum_{i=1}^{N}\exp[\sqrt{-1}2\pi(i-1)(k-1)/N]u'(i),\ k = 1,2,\ldots,N \tag{21}$$

Q.E.D.

References

1. W. F. Schreiber, T. S. Huang and O. J. Tretiak, "Contour Coding of Images," in Picture Bandwidth Compression, ed. by T. S. Huang and O. J. Tretiak, Gordon and Breach, NY, 1972.

2. T. S. Huang, "Coding of Two Tone Images," TR EE 77-10, School of Elec. Engr., Purdue University, W. Lafeyette, IN 47907.

3. A. Oosterlink, A. Reynaerts and H. Vanden Berghe, "Evaluation of different profile description and decomposition methods for banded chromosomes," Third Intl. Jt. Conf. on Patt. Recn., 1976, pp. 334-338.

4. H. Wechsler and J. Sklansky, "Finding the rib cage in chest radiographs," Pattern Recognition, Vol. 9, pp. 21-30, Jan. 1977.

5. A. Ambler et al., "A versatile computer controlled assembly system," Third Intl. Conf. on Art. Intel., 1973, pp. 298-303.

6. C. Rosen et al., "Exploratory research in advanced automation," Stanford Res. Inst., Aug. 1976.

7. G. H. Granlund, "Fourier preprocessing for hand printed character recognition," IEEE Trans. Computers, Vol. C-21, pp. 195-201, Feb. 1972.

8. C. T. Zahn and R. S. Roskies, "Fourier descriptors for plane closed curves," IEEE Trans. Computers, Vol. C-21, pp. 269-291, March 1972.

9. C. W. Richard and H. Hemami, "Identification of three-dimensional objects using Fourier descriptors of the boundary curve," IEEE Trans. Syst., Man, Cybern., Vol. SMC-4, pp. 371-378, July 1974.

10. E. Persoon and K. S. Fu, "Shape discrimination using Fourier descriptors," IEEE Trans. Syst., Man, Cybern., Vol. SMC-7, pp. 170-179, March 1977.

11. R. Bellman, "Introduction to Matrix Analysis," McGraw Hill, New York, 1960.

12. R. L. Kashyap and A. R. Rao, "Dynamic Stochastic Models from Empirical Data," Academic Press, New York, 1976.

13. R. L. Kashyap, "Optimal feature selection and decision rules in classification problems with time series," IEEE Trans. Information Theory, Vol. IT-24, pp. 281-288, May 1978.

14. R. L. Kashyap, "A Bayesian comparison of different classes of dynamic models using empirical data," IEEE Trans. Automat. Control, Vol. AC-22, pp. 715-727, Oct. 1977.

15. S. Impedovo et al., "A Fourier descriptor set for recognizing non-stylized numerals," IEEE Trans. Syst., Man, Cybern., Vol. SMC-8, pp. 640-645, August 1978.

16. B. Shapiro, "The use of orthogonal expansions for biological shape description," TR-472, Computer Science Center, Univ. of Md., College Park, MD 20742.

17. T. Pavlidis, "Structural Pattern Recognition," Springer-Verlag, New York, 1977.

18. D. N. Graham, "Image transmission by two-dimensional contour coding," Proc. IEEE, Vol. 55, pp. 336-346, March 1967.

19. J. W. Bacus and E. E. Gose, "Leucocyte pattern recognition," IEEE Trans. Syst., Man, Cybern., Vol. SMC-2, pp. 513-526, Sept. 1972.

20. I. T. Young et al., "An Analysis Technique for for Biological Shape 1," Information and Control, Vol. 25, pp. 357-370, Aug. 1974.

UNCLASSIFIED

SECURITY CLASSIFICATION OF THIS PAGE (When Data Entered)

REPORT DOCUMENTATION PAGE		READ INSTRUCTIONS BEFORE COMPLETING FORM
1. REPORT NUMBER	2. GOVT ACCESSION NO. AD-A089 843	3. RECIPIENT'S CATALOG NUMBER
4. TITLE (and Subtitle) STOCHASTIC MODELS FOR CLOSED BOUNDARY ANALYSIS: PART I - REPRESENTATION AND RECONSTRUCTION		5. TYPE OF REPORT & PERIOD COVERED Technical
		6. PERFORMING ORG. REPORT NUMBER TR-909
7. AUTHOR(s) R. L. Kashyap and R. Chellappa		8. CONTRACT OR GRANT NUMBER(s) AFOSR-77-3271
9. PERFORMING ORGANIZATION NAME AND ADDRESS Computer Vision Laboratory, Computer Science Center, University of Maryland, College Park, MD 20742		10. PROGRAM ELEMENT, PROJECT, TASK AREA & WORK UNIT NUMBERS
11. CONTROLLING OFFICE NAME AND ADDRESS Math. & Info. Sciences, AFOSR/NM Bolling AFB Wash., DC 20332		12. REPORT DATE July 1979
		13. NUMBER OF PAGES 39
14. MONITORING AGENCY NAME & ADDRESS(if different from Controlling Office)		15. SECURITY CLASS. (of this report) Unclassified
		15a. DECLASSIFICATION/DOWNGRADING SCHEDULE

16. DISTRIBUTION STATEMENT (of this Report)

Approved for public release; distribution unlimited.

17. DISTRIBUTION STATEMENT (of the abstract entered in Block 20, if different from Report)

18. SUPPLEMENTARY NOTES

19. KEY WORDS (Continue on reverse side if necessary and identify by block number)

Planar shape description
Image processing
Pattern recognition
Pattern analysis
Pattern synthesis
Contour coding
Stochastic models

20. ABSTRACT (Continue on reverse side if necessary and identify by block number)

This paper deals with the analysis of closed boundaries of arbitrary shape in a plane. Specifically, it is concerned with the problems of representation and reconstruction. We first set up a one to one correspondence between the given closed boundary and a univariate or multivariate sequence of real numbers. Univariate or multivariate circular autoregressive models are suggested for the representation of the sequence of numbers derived from the closed boundary. The stochastic model representing the

DD FORM 1 JAN 73 1473 EDITION OF 1 NOV 65 IS OBSOLETE

UNCLASSIFIED

SECURITY CLASSIFICATION OF THIS PAGE (When Data Entered)

closed boundary is invariant to transformations of the boundary such as scaling, rotation and choice of the starting point. Methods for estimating the unknown parameters of the model are given and a decision rule for choosing the appropriate order of the model is included. Constraints on the estimates are derived so that the estimates are invariant to transformations of the boundaries. The specific stochastic model used enables us to reconstruct a closed boundary with less computational effort using FFT algorithms. Results of simulations are included and applications to contour coding are discussed. In a subsequent paper we will consider the classification problem.

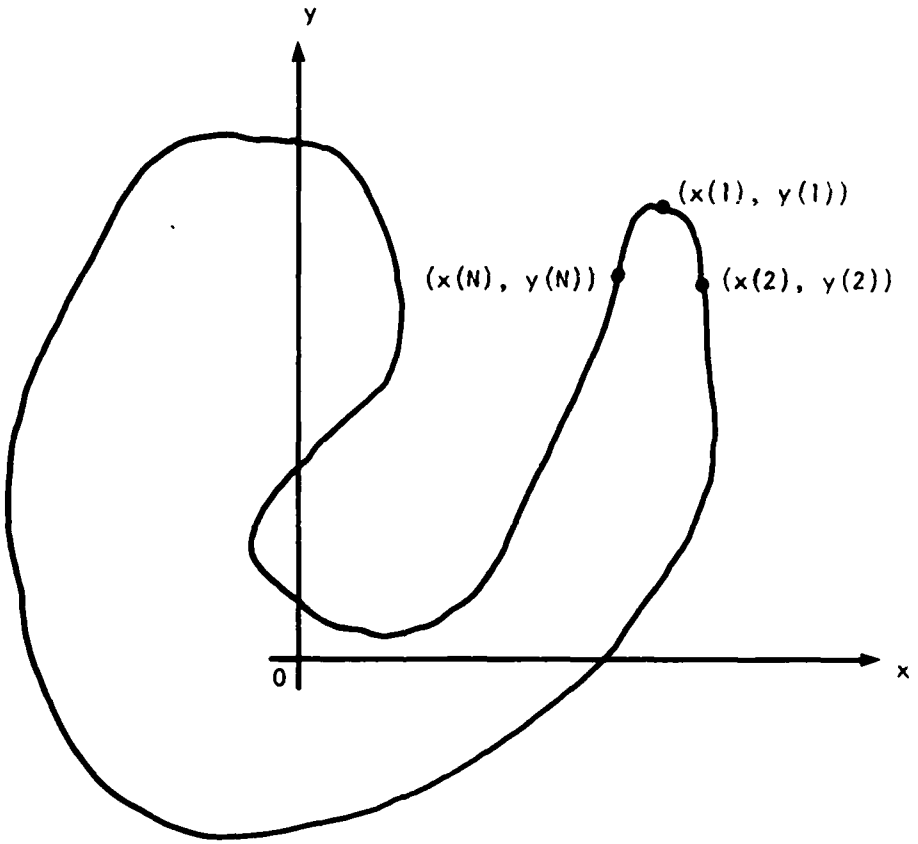

Fig. 1. Two dimensional representation.

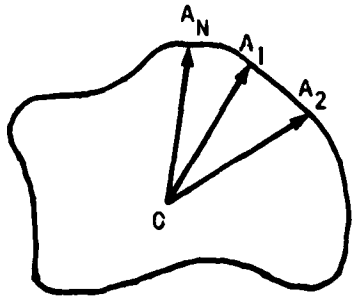

Fig. 2. One dimensional representation.

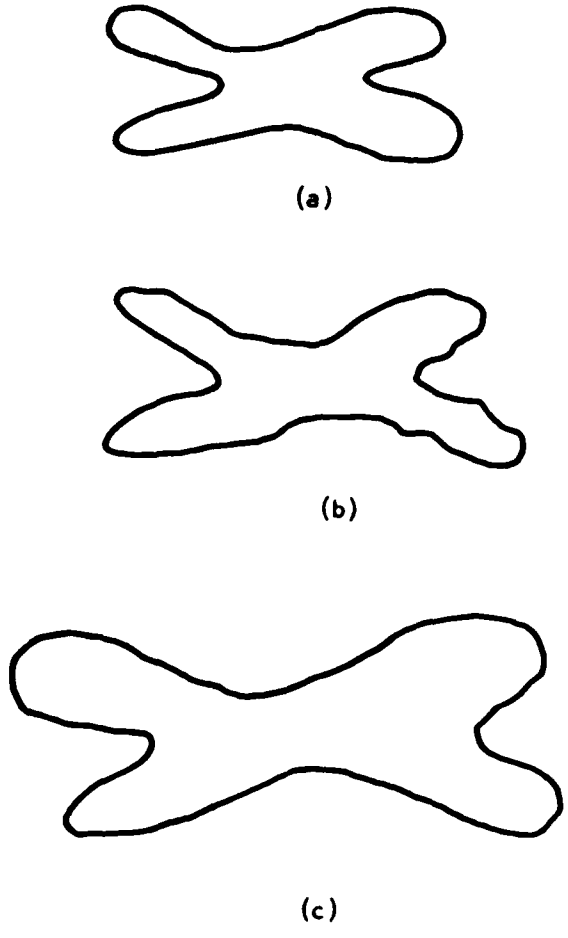

Fig. 3. Variations in shape: a) original shape, b) noisy shape (local transformations), c) original shape globally transformed (scaling).

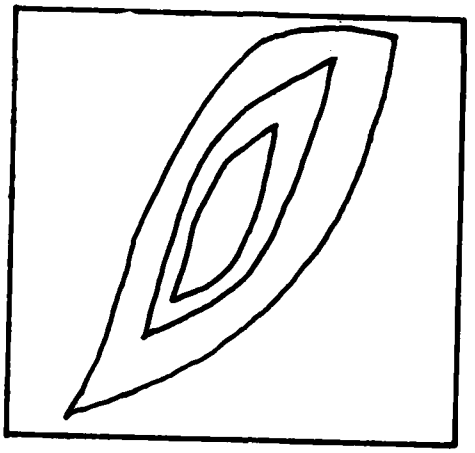

Fig. 4. Contour maps.

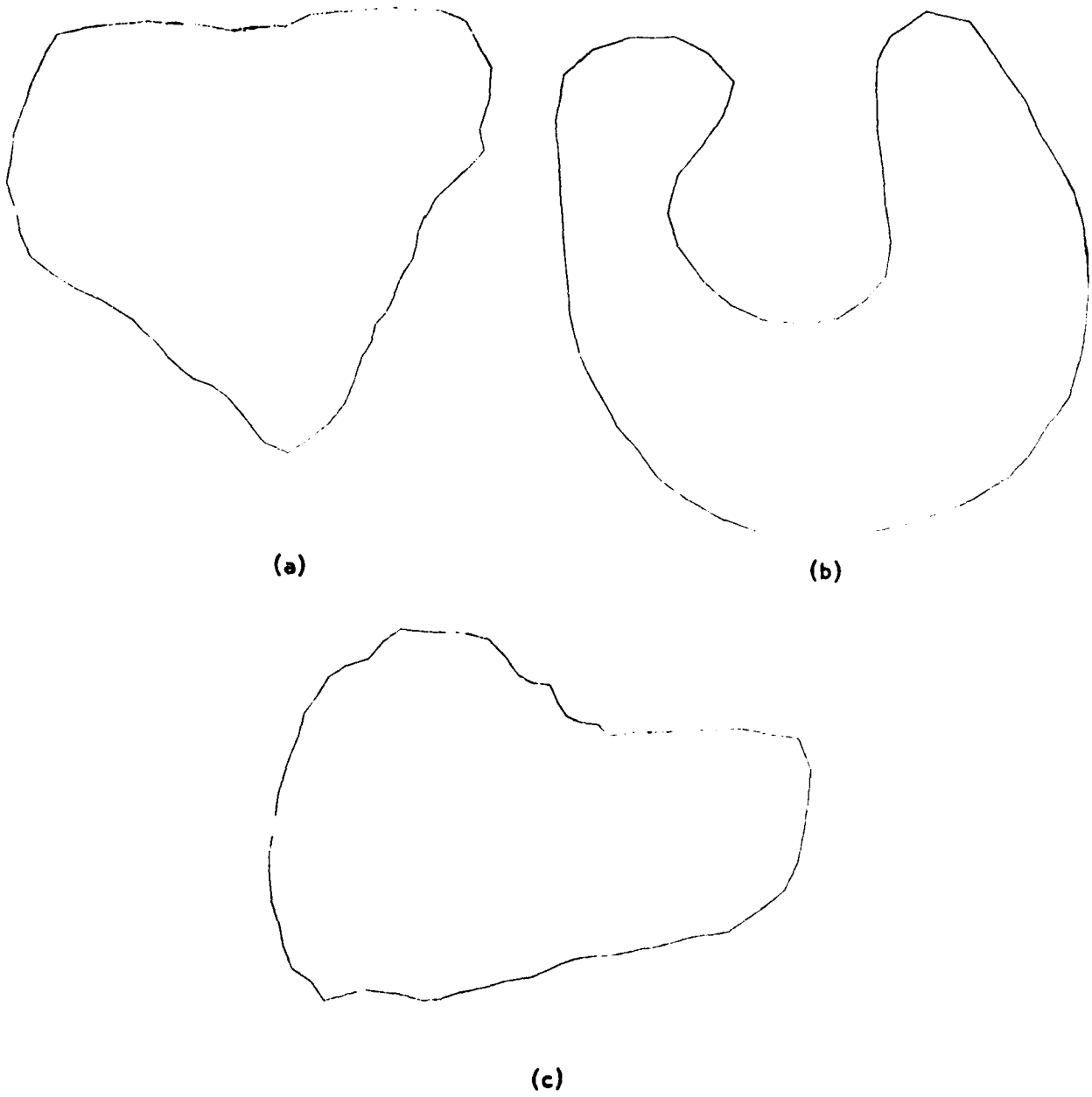

Fig. 5. Closed boundaries considered in the simulation: a) shape A, b) shape B, c) shape C.

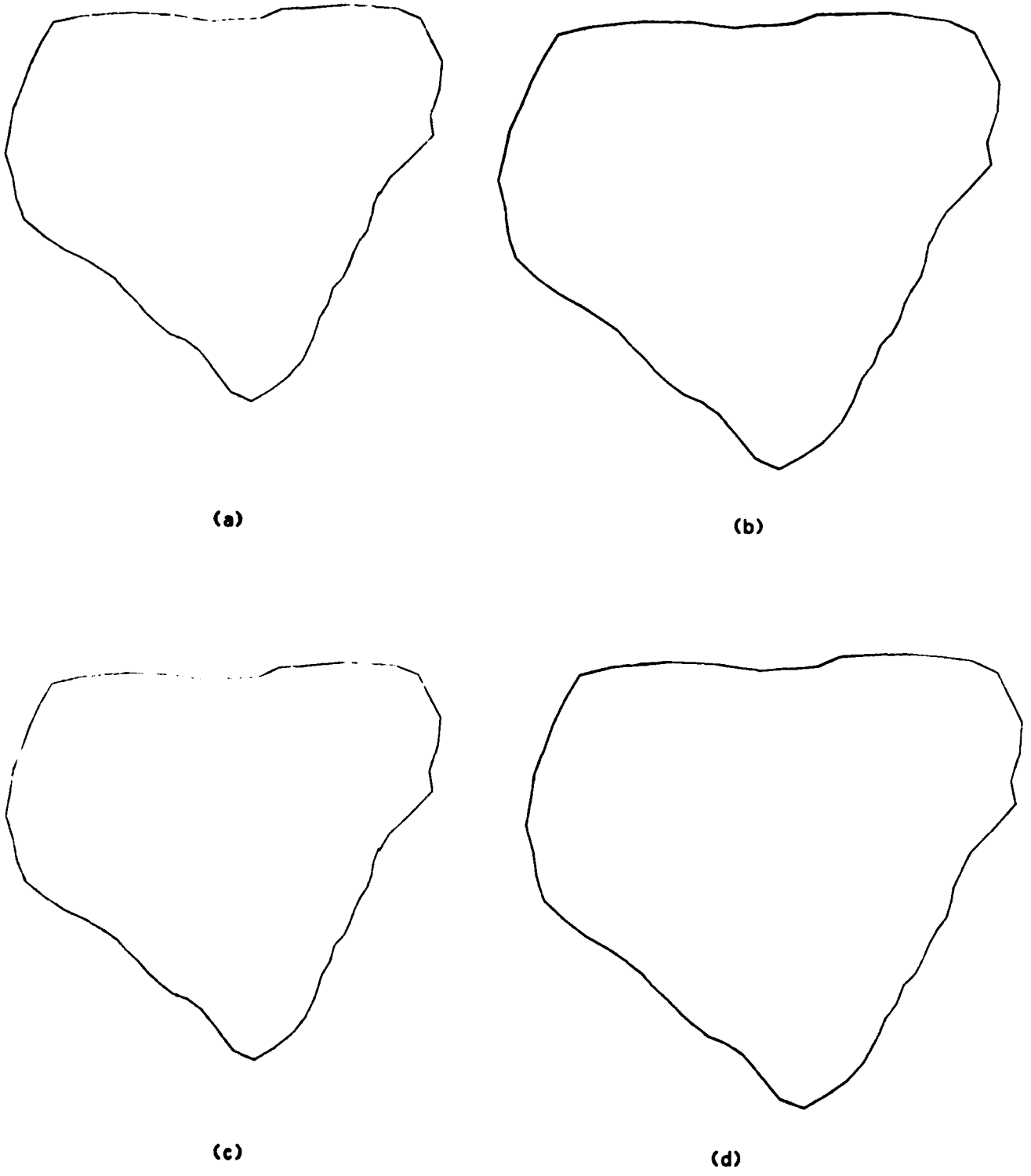

Fig. 6. Reconstruction of shape A using the simultaneous scheme. a) m=2 with exact residuals, b) m=2 with residuals truncated to first decimal place, c) similar to a) with m=12, d) similar to b) with m=12. Note that b) and d) are close to the original.

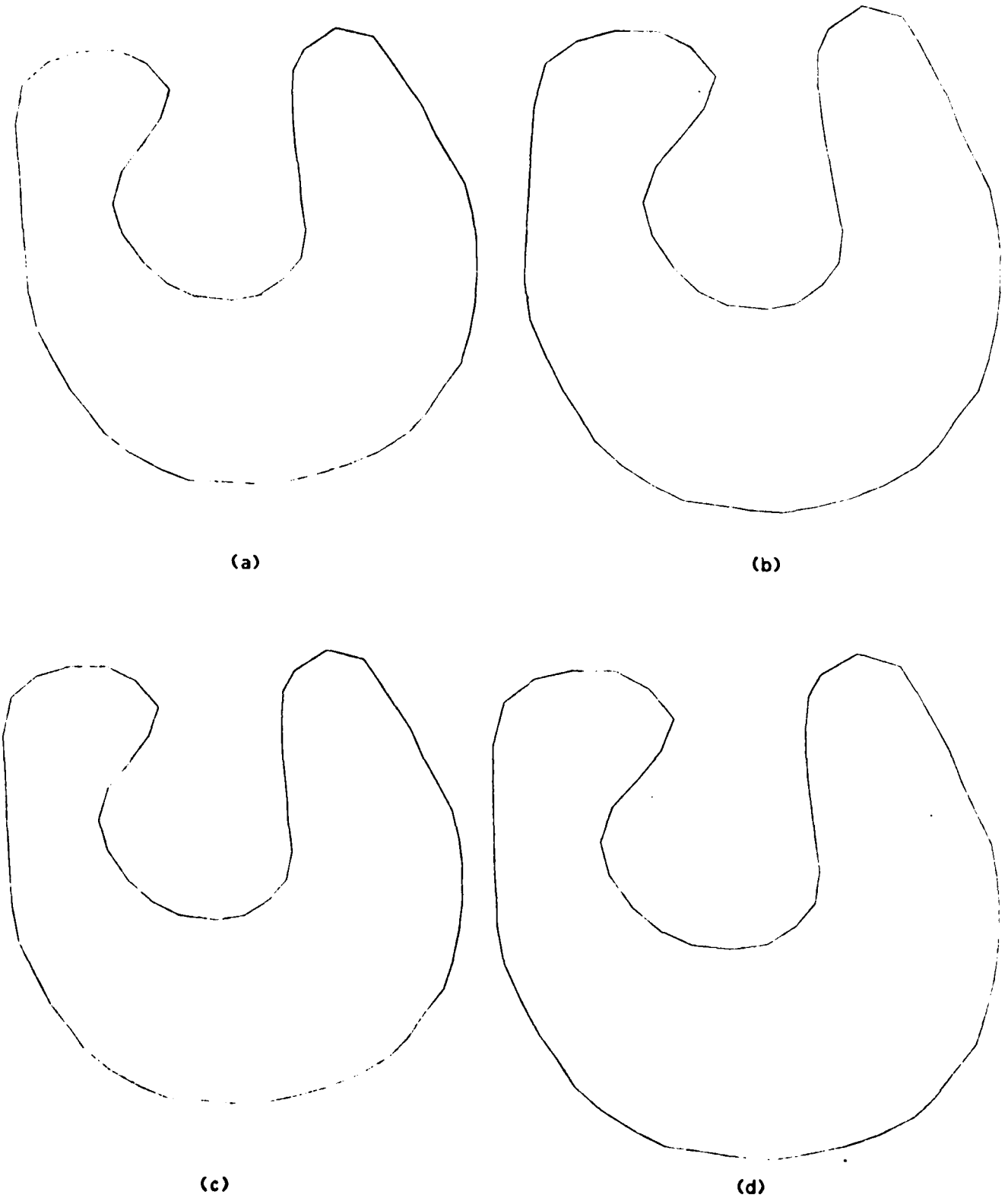

Fig. 7. Reconstruction of shape B using the simultaneous scheme. a) m=2 with exact residuals, b) m=2 with residuals truncated to first decimal place, c) similar to a) with m=12, d) similar to b) with m=12. Note that b) and d) are close to the original.

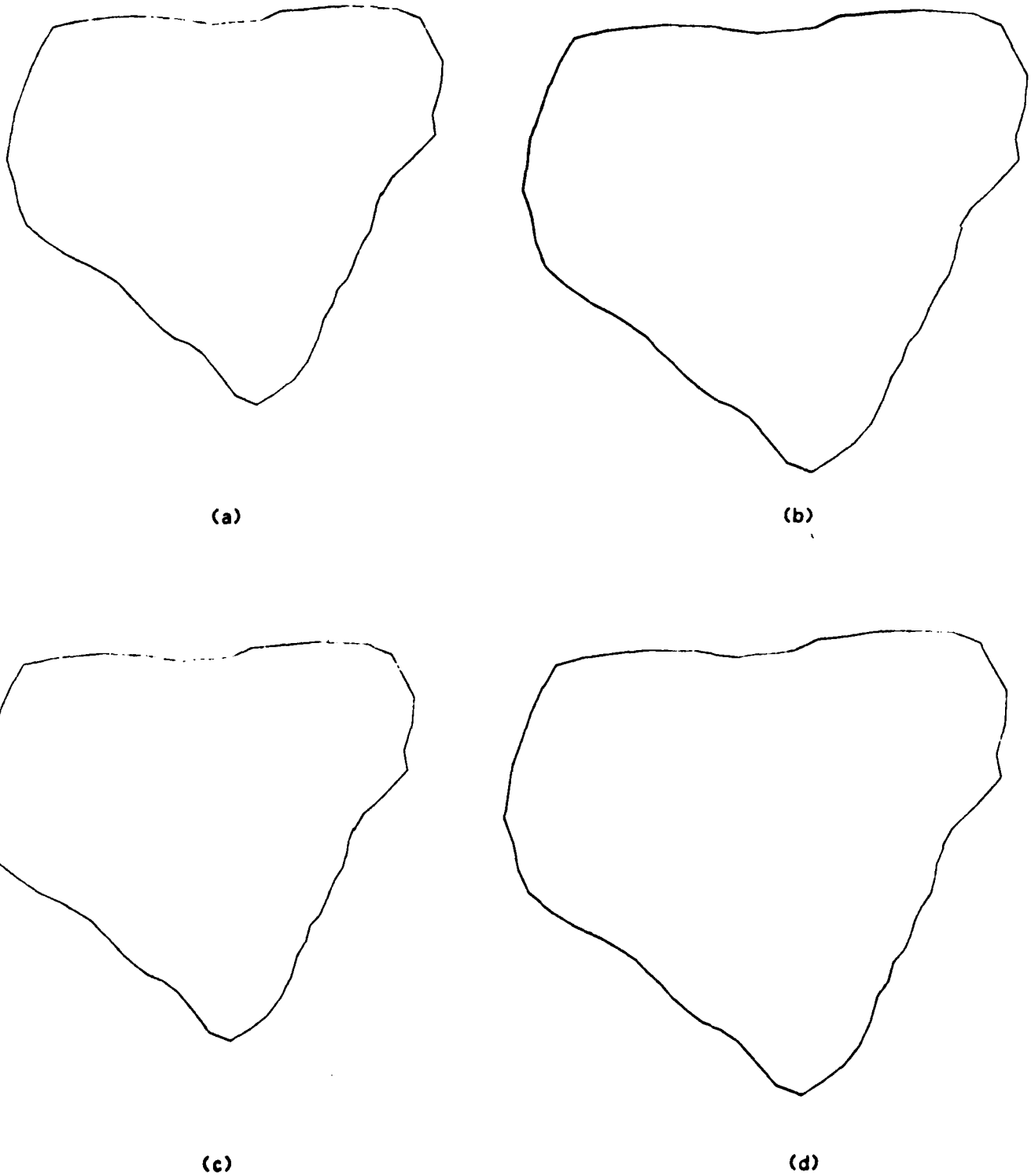

Fig. 8. Reconstruction of shape A using the recursive scheme. a) m=2 with exact residuals, b) m=2 with residuals truncated to first decimal place, c) similar to a) with m=12, d) similar to b) with m=12.

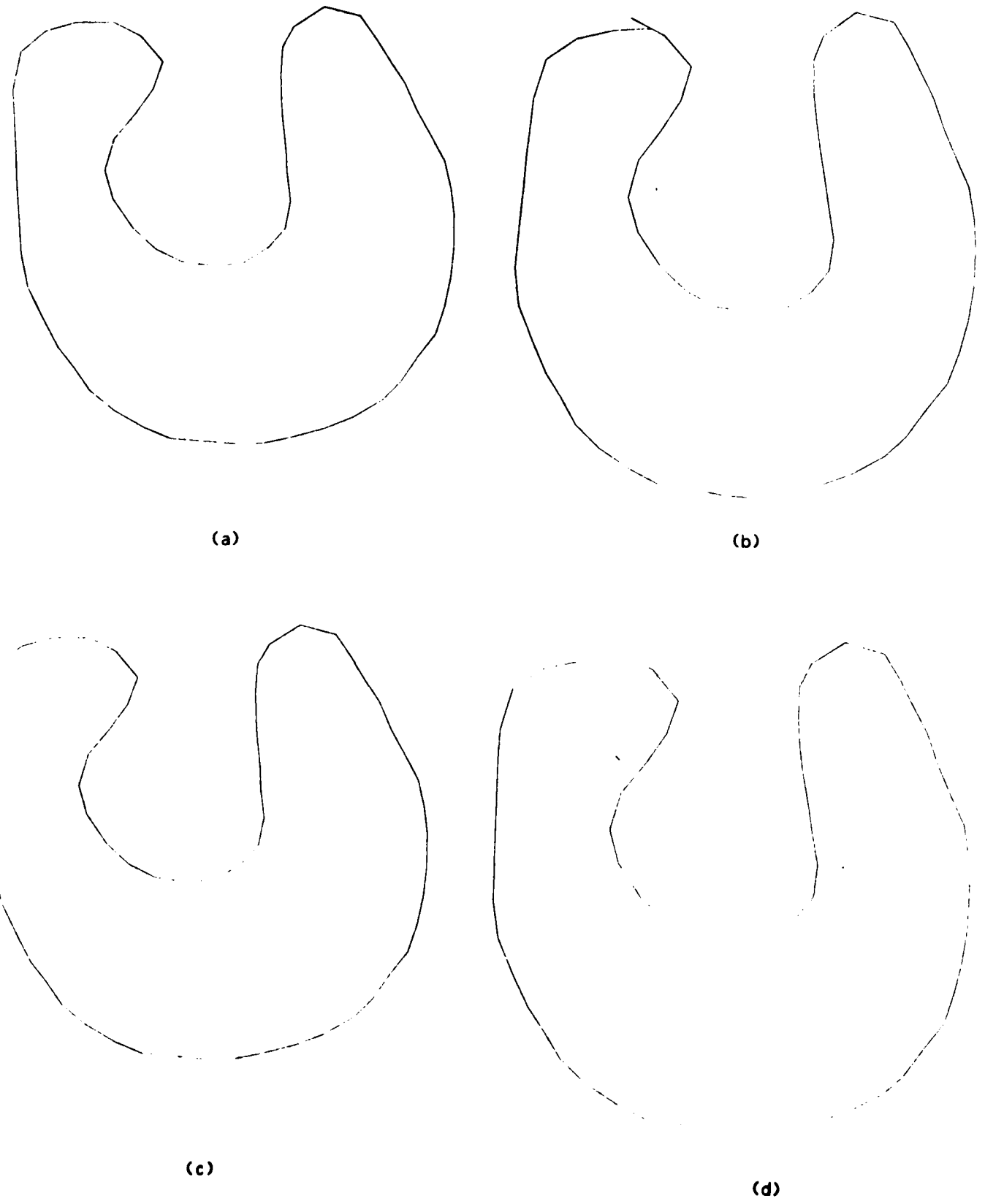

Fig. 9. Reconstruction of shape B using the recursive scheme. a) m=2 with exact residuals, b) m=2 with residuals truncated to first decimal place (note the spike), c) similar to a) with m=12, d) similar to b) with m=12 (note that the reconstructed contour is not closed).

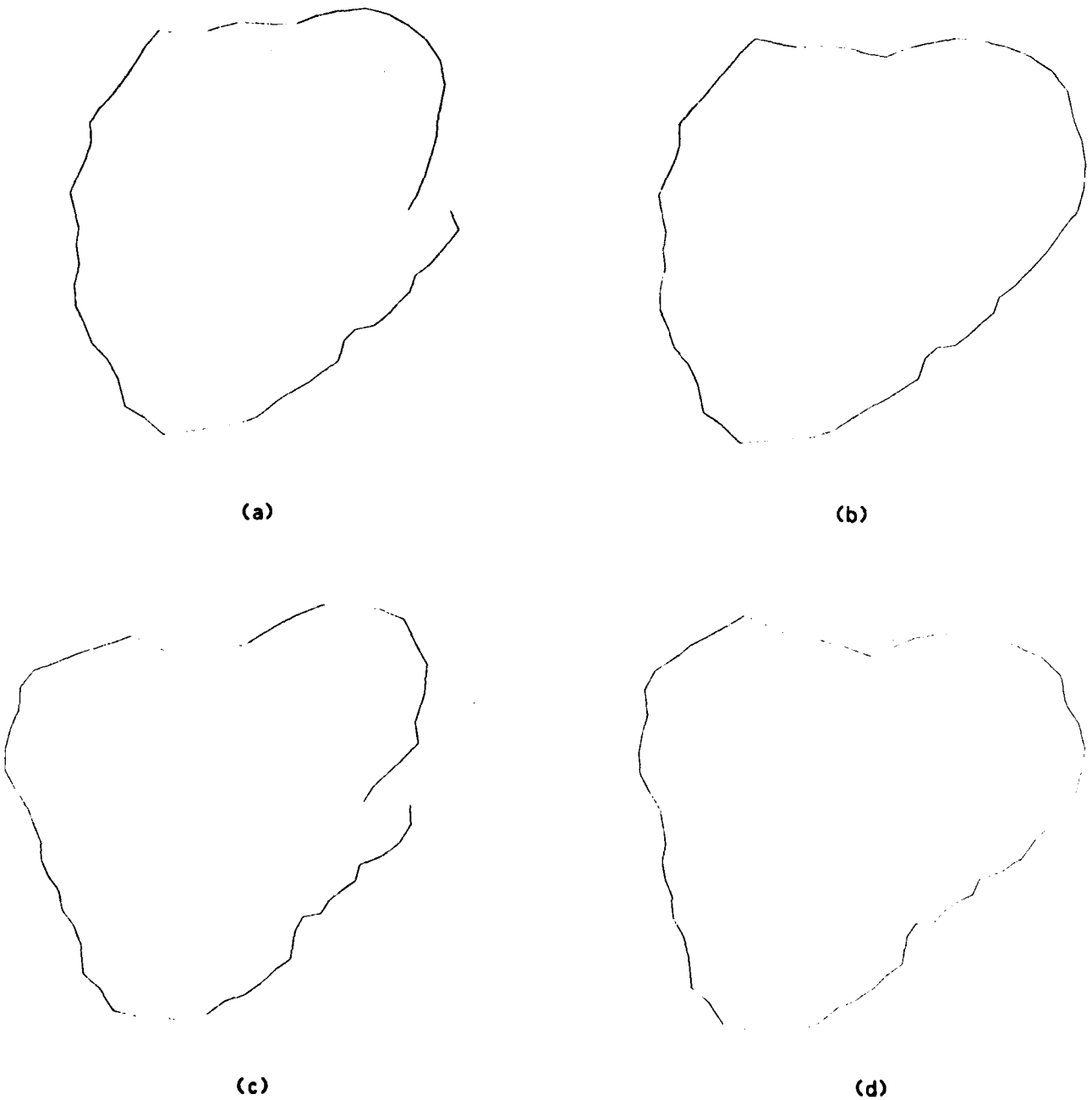

Fig. 10. Synthetic generation of shape A with residuals drawn from a (0 1) pseudorandom Gaussian generator. a) m=2 with recursive scheme, b) m=2 with simultaneous scheme, c) similar to a) with m=12, d) similar to b) with m=12. Note that the contours constructed with the recursive scheme are not closed.

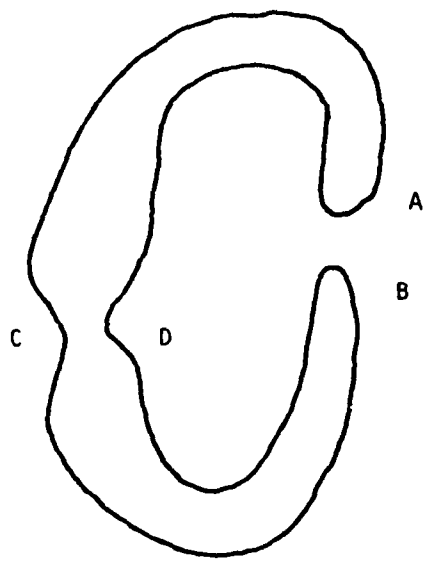

Fig. 11. Shapes with necks.

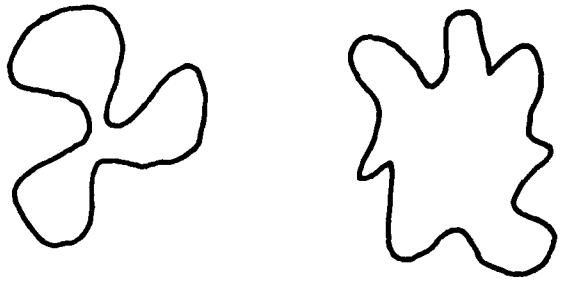

Fig. 12. Non-robustness of shape descriptor P^2/A, P = perimeter, A = area [19].

UNCLASSIFIED

SECURITY CLASSIFICATION OF THIS PAGE *(When Data Entered)*

REPORT DOCUMENTATION PAGE	READ INSTRUCTIONS BEFORE COMPLETING FORM
1. REPORT NUMBER **AFOSR-TR- 80-0946** 2. GOVT ACCESSION NO. AD-A094843	3. RECIPIENT'S CATALOG NUMBER
4. TITLE *(and Subtitle)* STOCHASTIC MODELS FOR CLOSED BOUNDARY ANALYSIS: PART I-REPRESENTATION AND RECONSTRUCTION	5. TYPE OF REPORT & PERIOD COVERED Interim 6. PERFORMING ORG. REPORT NUMBER
7. AUTHOR(s) R. L. Kashyap R. Chellappa	8. CONTRACT OR GRANT NUMBER(s) AFOSR 77-3271
9. PERFORMING ORGANIZATION NAME AND ADDRESS University of Maryland Computer Science Center College Park, MD 20742	10. PROGRAM ELEMENT, PROJECT, TASK AREA & WORK UNIT NUMBERS 61102F 2304/A2
11. CONTROLLING OFFICE NAME AND ADDRESS Air Force Office of Scientific Research/NM Bolling AFB, Washington, DC 20332	12. REPORT DATE July 1980 13. NUMBER OF PAGES 51
14. MONITORING AGENCY NAME & ADDRESS *(if different from Controlling Office)*	15. SECURITY CLASS. *(of this report)* UNCLASSIFIED 15a. DECLASSIFICATION DOWNGRADING SCHEDULE

16. DISTRIBUTION STATEMENT *(of this Report)*

Approved for public release; distribution unlimited.

17. DISTRIBUTION STATEMENT *(of the abstract entered in Block 20, if different from Report)*

18. SUPPLEMENTARY NOTES

19. KEY WORDS *(Continue on reverse side if necessary and identify by block number)*

Planar shape discription
Image processing
Pattern recognition
Pattern analysis
Pattern synthesis
Contour coding
Stochastic models

20. ABSTRACT *(Continue on reverse side if necessary and identify by block number)*

This paper deals with the analysis of closed boundaries of arbitrary shape in a plane. Specifically, it is concerned with the problems of representation and reconstruction. We first set up a one to one correspondence between the given closed boundary and a univariate or multivariate sequence of real numbers. Univariate or multivariate circular autoregressive models are suggested for the representation of the sequence of numbers derived from the closed boundary. The stochastic model representing the closed boundary is invariant to transformations of the boundary such as scaling, rotation and choice of the starting point. Methods

DD FORM 1 JAN 73 1473 EDITION OF 1 NOV 65 IS OBSOLETE

UNCLASSIFIED

SECURITY CLASSIFICATION OF THIS PAGE *(When Data Entered)*

20. Abstract cont.

for estimating the unknown parameters of the model are given and a decision rule for chocsing the appropriate order of the model is included. Constraints on the estimates are derived so that the estimates are invariant to transformations of the boundaries. The specific stochastic model used enables us to reconstruct a closed boundary with less computational effort using FFT algorithms. Results of simulations are included and applications to contour coding are discussed. In a subsequent paper we will consider the classification problem.